A&A 372, 1078–1082 (2001)
DOI: 10.1051/0004-6361:20010565

Astronomy & Astrophysics

Atomic data from the IRON Project

XLIX. Electron impact excitation of Fe XX*

K. Butler[1] and C. J. Zeippen[2]

[1] Institut für Astronomie und Astrophysik, Scheinerstr. 1, 81679 München, Germany
[2] UMR 8631 (associée au CNRS et à l'Université Paris 7) et DAEC, Observatoire de Paris, 92195 Meudon, France

Received 22 January 2001 / Accepted 12 April 2001

Abstract. Collisional data between 86 levels of the $n = 2$ and $n = 3$ complexes of N-like iron are presented. The data have been obtained in a Breit-Pauli relativistic approximation and include resonance contributions by the use of close-coupling wavefunctions. The R-matrix package described by Hummer et al. (1993) has been used to solve the close-coupling equations at several thousand energy points for an extensive target leading to collision strengths accurate to better than 20%.

Key words. atomic data

1. Introduction

The calculation of atomic data for highly ionized species of the iron group elements has been stimulated by solar studies. In particular, accurate collisional data are necessary for the intepretation of coronal spectra, allowing the physical properties of the corona to be determined. This in turn provides important information about the heating mechanisms in the sun and its outer layers. The pioneering work on Fe XX, the ion to be discussed here, was performed by Bhatia & Mason (1980) and Mason & Bhatia (1983). It was initiated as a response to the SMM (Solar Maximum Mission) observations of Phillips et al. (1982). The present calculations are a part of the Iron Project (Hummer et al. 1993), an international project set up to provide accurate atomic data for the analysis of data obtained by the SOHO solar satellite and by the new generation of X-ray satellites which have recently become reality with the launch of the XMM and Chandra satellites, late in 1998.

The early calculations were based on the distorted wave (DW) approximation which is well suited to these highly ionized systems and is relatively simple to carry out. It is deficient, however, in that it omits the coupling between the various scattering electron + target system combinations (the channels) which leads to large resonance contributions to the collision rates. The "close-coupling" method used here includes these couplings but is correspondingly more costly to perform. The collisional cross sections vary rapidly in energy, making a fine grid necessary whereas Bhatia & Mason (1980) tabulate results at three energies and Mason & Bhatia (1983) give results at a single incident electron energy since their cross sections are slowly varying. The R-matrix technique of Berrington et al. (1978) has proven to be invaluable in this regard since a single diagonalization of the scattering system Hamiltonian allows the collisional cross sections at a large number of energies to be obtained relatively cheaply. The goals and methods of the Iron Project are summarized in the introductory paper by Hummer et al. (1993) while more information is to be found on the project home page at

`http://www.usm.uni-muenchen.de/ ...`
`... people/ip/iron-project.html`

Recently, Zhang & Sampson (1999) have produced relativistic DW collisional data for the $n = 2$ transitions of all N-like ions satisfying $12 < Z < 92$, including Fe XX. While their data also lack resonant contributions, these and the earlier distorted wave results do provide a useful check on the convergence of the present data with regard to partial waves and the accuracy of the approximations as a whole. At the same time our results provide a spot check on the extensive tabulations of Zhang and Sampson.

The paper is organized as follows. The next section gives a brief summary of the methods involved and provides some indication as to the accuracy of the target

Send offprint requests to: K. Butler,
e-mail: `butler@usm.uni-muenchen.de`

* Detailed tables of the present data are available in electronic form at the CDS via anonymous ftp to `cdsarc.u-strasbg.fr` (`ftp 130.79.128.5`) or via `http://cdsweb.u-strasbg.fr/cgi-bin/qcat?J/A+1/372/1078`

wavefunctions. In Sect. 3, we present the collisional cross sections and compare with previous work. We also summarize our results and give an overview of our future plans.

2. Method

The "standard" methods described in detail by Hummer et al. (1993) have been used in deriving the collisional data presented here. In particular, we follow closely the approach delineated in our previous paper on C-like iron (Butler & Zeippen 2000) both in the target description and in the numerical treatment. Here we present only the specific details relevant to the present N-like iron system.

The target consists of 12 configurations comprising all of the $n = 2$ and the energetically lowest of the $n = 3$ configurations.

Table 1. The target configurations used for Fe XX.

$2s^22p^3$	$2s2p^4$	$2p^5$
$2s^22p^23s$	$2s^22p^23p$	$2s^22p^23d$
$2s2p^33s$	$2s2p^33p$	$2s2p^33d$
$2p^43s$	$2p^43p$	$2p^43d$

All the target calculations were performed using a version of the program SUPERSTRUCTURE (Eissner et al. 1974) due to Nussbaumer & Storey (1978). Energy levels of $2s^22p^3$, $2s2p^4$, $2p^5$, $2s^22p^23s$, $2s^22p^23p$, $2s^22p^23d$ together with a small number of interposing levels from the $2s2p^33s$ and $2s2p^33p$ configurations have been included explicitly in the target description leading to a total of 86 target states. The lambda parameters of a set of Thomas-Fermi-Dirac-Almadi potentials were determined by minimizing the weighted energy sum of all the levels of all the configurations to obviate possible problems with pseudoresonances and are presented in Table 2. The wavefunctions are of good quality, as the comparison of the observed and calculated energies in Table 3 demonstrate. In all cases, the agreement is better than 5%.

This is further confirmed in Figs. 1 and 2 in which the present oscillator strengths are compared with those of Bhatia & Mason (1980) and Mason & Bhatia (1983), their case B) and of Zhang & Sampson (1999). Again, the agreement is good. There are some discrepancies for the $n = 3$ states. This is mostly caused by configurational mixing of the higher lying levels which are therefore less accurately represented than the $n = 2$ states. This is clear from the figures as Zhang & Sampson only considered the $n = 2$ levels where the agreement is excellent. The overall

Table 2. The λ parameters for Fe XX.

$n\ell$	$\lambda_{n\ell}$	$n\ell$	$\lambda_{n\ell}$
1s	1.41988	3s	1.24555
2s	1.35297	3p	1.19944
2p	1.27405	3d	1.29366

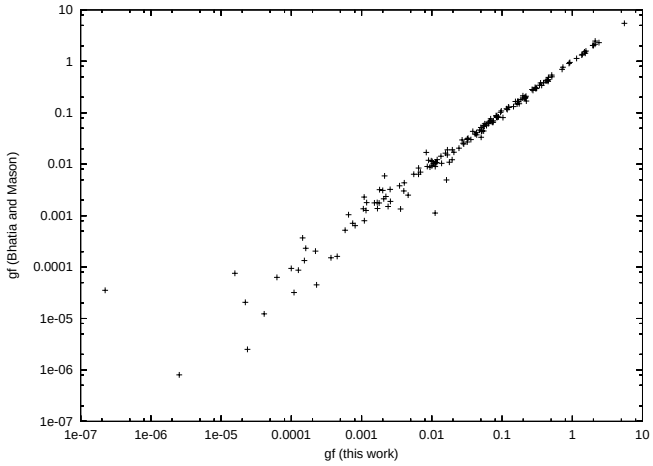

Fig. 1. Comparison of the gf-values obtained in the present Fe XX target calculation with those of Bhatia & Mason (1980) and Mason & Bhatia (1983).

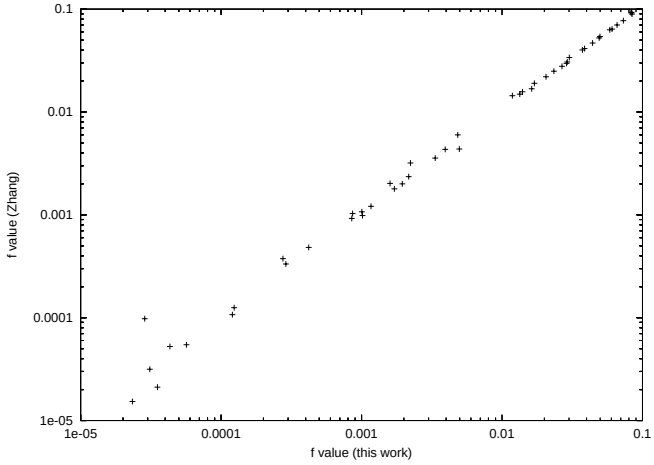

Fig. 2. Comparison of the f-values obtained in the present Fe XX target calculation with those of Zhang & Sampson (1999).

accuracy of the target wavefunctions is thus confirmed. The present f-values are tabulated in Table 5 which is only available in electronic form. They provide the high energy and temperature limits of the collision strengths and rates of the allowed transitions (see e.g. Burgess & Tully 1992).

These wavefunctions have been utilized to provide the target for a close-coupling calculation in a Breit-Pauli approximation. An unpublished R-matrix package due to Eissner based on the programs described by Berrington et al. (1995) was used for this purpose. Values of the total angular momentum J up to $J = 28$ have been considered ensuring convergence in J in most of the transitions. The remainder have been "topped-up" using a geometric progression or the Coulomb-Bethe approximation as implemented by Eissner et al. (1999) for intermediate coupling. This procedure is based on the work of Burke & Seaton (1986) for the LS-coupling case and accounts for the sum to infinity in J for the allowed transitions. The use of these

Table 3. Calculated versus observed (Sugar & Corliss 1985) target energies (cm^{-1}).

Index	Term		E_{calc}	E_{obs}	Index	Term		E_{calc}	E_{obs}
1	$2s^22p^3$	$^4S^o_{3/2}$	0.	0.	44	$2s^22p^23p$	$^2P^o_{1/2}$	7696319.	
2	$2s^22p^3$	$^2D^o_{3/2}$	142083.	138620.	45	$2s^22p^23d$	$^2P^e_{3/2}$	7730619.	
3	$2s^22p^3$	$^2D^o_{5/2}$	183972.	176130.	46	$2s^22p^23d$	$^4F^e_{7/2}$	7732553.	
4	$2s^22p^3$	$^2P^o_{1/2}$	264485.	260270.	47	$2s^22p^23d$	$^4D^e_{1/2}$	7737390.	
5	$2s^22p^3$	$^2P^o_{3/2}$	329746.	323340.	48	$2s^22p^23d$	$^4D^e_{5/2}$	7740964.	
6	$2s2p^4$	$^4P^e_{5/2}$	757309.	752730.	49	$2s^22p^23p$	$^2P^o_{3/2}$	7752010.	
7	$2s2p^4$	$^4P^e_{3/2}$	825299.	820820.	50	$2s^22p^23d$	$^4D^e_{3/2}$	7765580.	
8	$2s2p^4$	$^4P^e_{1/2}$	847488.	842740.	51	$2s^22p^23d$	$^4D^e_{7/2}$	7769297.	
9	$2s2p^4$	$^2D^e_{3/2}$	1055924.	1042570.	52	$2s^22p^23d$	$^2F^e_{5/2}$	7770931.	
10	$2s2p^4$	$^2D^e_{5/2}$	1074138.	1058360.	53	$2s^22p^23d$	$^4F^e_{9/2}$	7772757.	
11	$2s2p^4$	$^2S^e_{1/2}$	1209106.	1195260.	54	$2s2p^33s$	$^4S^o_{3/2}$	7773517.	
12	$2s2p^4$	$^2P^e_{3/2}$	1260657.	1242430.	55	$2s^22p^23p$	$^2P^o_{1/2}$	7791773.	
13	$2s2p^4$	$^2P^e_{1/2}$	1359453.	1340040.	56	$2s^22p^23d$	$^4P^e_{5/2}$	7805476.	7802000.
14	$2p^5$	$^2P^o_{3/2}$	1980580.	1954520.	57	$2s^22p^23p$	$^2P^o_{3/2}$	7805415.	
15	$2p^5$	$^2P^o_{1/2}$	2092435.	2062200.	58	$2s^22p^23d$	$^4P^e_{3/2}$	7817016.	7802000.
16	$2s^22p^23s$	$^4P^e_{1/2}$	7175982.		59	$2s^22p^23d$	$^2P^e_{1/2}$	7819123.	
17	$2s^22p^23s$	$^4P^e_{3/2}$	7241261.		60	$2s^22p^23d$	$^4P^e_{1/2}$	7825962.	
18	$2s^22p^23s$	$^2P^e_{1/2}$	7272599.		61	$2s^22p^23d$	$^2F^e_{7/2}$	7840322.	7820000.
19	$2s^22p^23s$	$^4P^e_{5/2}$	7285832.		62	$2s2p^33p$	$^6P^e_{3/2}$	7862699.	
20	$2s^22p^23s$	$^2P^e_{3/2}$	7318300.		63	$2s^22p^23d$	$^2D^e_{3/2}$	7864236.	7859000.
21	$2s^22p^23p$	$^4D^o_{1/2}$	7377179.		64	$2s^22p^23d$	$^2D^e_{5/2}$	7866320.	7843000.
22	$2s^22p^23p$	$^4D^o_{3/2}$	7419637.		65	$2s2p^33p$	$^6P^e_{5/2}$	7870585.	
23	$2s^22p^23s$	$^2D^e_{5/2}$	7420295.		66	$2s2p^33p$	$^6P^e_{7/2}$	7886943.	
24	$2s^22p^23s$	$^2D^e_{3/2}$	7430193.		67	$2s^22p^23d$	$^2G^e_{7/2}$	7903215.	
25	$2s^22p^23p$	$^2S^o_{1/2}$	7439068.		68	$2s^22p^23d$	$^2G^e_{9/2}$	7919633.	
26	$2s^22p^23p$	$^4P^o_{3/2}$	7468941.		69	$2s^22p^23d$	$^2D^e_{3/2}$	7932593.	7919000.
27	$2s^22p^23p$	$^4D^o_{5/2}$	7476966.		70	$2s^22p^23d$	$^2D^e_{5/2}$	7938076.	7913000.
28	$2s^22p^23p$	$^4P^o_{1/2}$	7489727.		71	$2s^22p^23d$	$^2P^e_{1/2}$	7952474.	
29	$2s^22p^23p$	$^4P^o_{5/2}$	7499471.		72	$2s2p^33p$	$^4P^e_{3/2}$	7953949.	
30	$2s^22p^23p$	$^2D^o_{3/2}$	7510143.		73	$2s2p^33p$	$^4P^e_{5/2}$	7954812.	
31	$2s^22p^23p$	$^4D^o_{7/2}$	7520954.		74	$2s^22p^23d$	$^2F^e_{7/2}$	7961359.	7935000.
32	$2s^22p^23p$	$^4S^o_{3/2}$	7544200.		75	$2s2p^33s$	$^4D^o_{3/2}$	7961796.	
33	$2s^22p^23s$	$^2S^e_{1/2}$	7544519.		76	$2s2p^33p$	$^4P^e_{1/2}$	7961540.	
34	$2s^22p^23p$	$^2P^o_{3/2}$	7569260.		77	$2s2p^33s$	$^4D^o_{1/2}$	7963390.	
35	$2s^22p^23p$	$^2D^o_{5/2}$	7574025.		78	$2s2p^33s$	$^4D^o_{5/2}$	7964406.	
36	$2s^22p^23p$	$^2P^o_{1/2}$	7593566.		79	$2s^22p^23d$	$^2S^e_{1/2}$	7986650.	
37	$2s2p^33s$	$^6S^o_{5/2}$	7643308.		80	$2s^22p^23d$	$^2P^e_{3/2}$	7988286.	7967000.
38	$2s^22p^23p$	$^2F^o_{5/2}$	7648196.		81	$2s^22p^23d$	$^2F^e_{5/2}$	7989414.	7983000.
39	$2s^22p^23d$	$^4F^e_{3/2}$	7657504.		82	$2s2p^33s$	$^4D^o_{7/2}$	7989648.	
40	$2s^22p^23p$	$^2F^o_{7/2}$	7661373.		83	$2s2p^33s$	$^2D^o_{3/2}$	8034063.	
41	$2s^22p^23p$	$^2D^o_{3/2}$	7670456.		84	$2s2p^33s$	$^2D^o_{5/2}$	8053000.	
42	$2s^22p^23d$	$^4F^e_{5/2}$	7681487.		85	$2s^22p^23d$	$^2D^e_{5/2}$	8065330.	8047000.
43	$2s^22p^23p$	$^4D^o_{5/2}$	7689671.		86	$2s^22p^23d$	$^2D^e_{5/2}$	8075937.	

procedures is discussed in our previous paper (Butler & Zeippen 2000) and will not be repeated here. It should be noted that these corrections are only of importance at high energies.

Collision strengths were obtained on a fine grid up to a maximum of 290 Ryd. Three different step lengths, 0.000003115 from 0.00394992 to 0.0533392, 0.0000474 from 0.0533392 up to the region of all channels open and 0.02 above, all in scaled Rydberg units (Ryd/z^2), were used to give good coverage of the resonances. These data were then convolved with a Maxwellian distribution to provide the effective collision strengths tabulated in

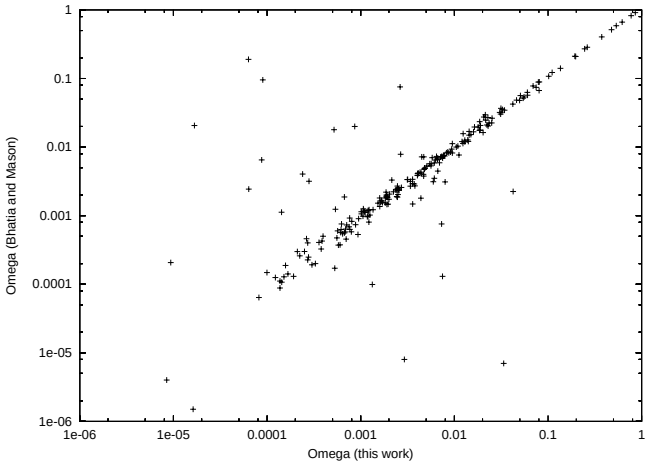

Fig. 3. Comparison of the collision strengths (Omega) obtained in the present calculation at an incident electron energy of 80 Ryd with those of Bhatia & Mason (1980) and Mason & Bhatia (1983).

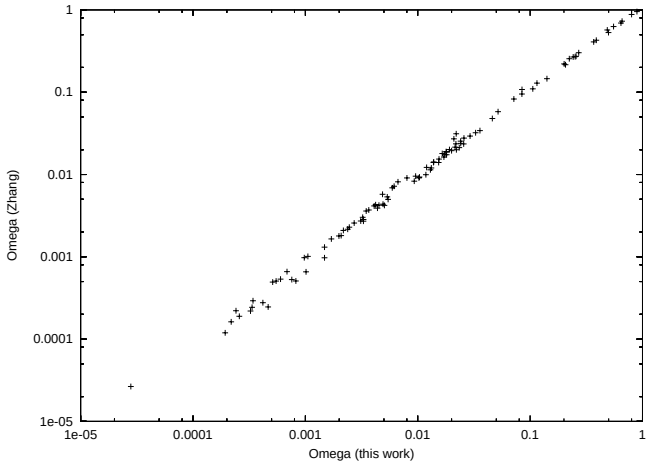

Fig. 4. Comparison of the collision strengths (Omega) obtained in the present calculation at an ejected electron energy of 88.2 Ryd with those of Zhang & Sampson (1999).

Table 4. Data for transitions between the lowest 15 levels at $\log T = 6.9$, corresponding to the maximum abundance of this ion according to Arnaud & Rothenflug (1985), are given. The remaining data are available electronically from the CDS via anonymous `ftp 130.79.128.5`. Care was taken in performing the integration to ensure that the correct low temperature limit was attained as described by Burgess & Tully (1992). Data are presented for logarithmic temperatures from 5.0 to 7.3 in steps of 0.1 covering the maximum ionic abundance according to Arnaud & Rothenflug (1985). The contribution from energies above the maximum (290 Ryd) is negligible for all but the highest temperatures considered here. This contribution has been taken into account by simply extrapolating the last calculated value to higher energies. While this procedure is crude the error involved is in all cases smaller than the estimated overall error.

3. Results and discussion

We begin by considering high energies where the distorted wave and the close-coupling results should be similar. Here we can compare both with the data provided by Bhatia & Mason (1980), Mason & Bhatia (1983) and Zhang & Sampson (1999). This has been done in Figs. 3 and 4 respectively. In Fig. 3, we compare the present and earlier results for all common transitions at an incident electron energy of 80 Ryd (we linearly interpolated the Bhatia and Mason data from the tabulated values at 50 and 100 Ryd). The agreement is good overall with some larger discrepancies for the $n = 3$ transitions, as is evidenced by the excellent agreement with Zhang & Sampson (1999) for the $n = 2$ transitions shown in Fig. 4. The differences are due to the target descriptions where we have more configuration interaction compared to the work of Mason & Bhatia (1983). The $2s2p^3 3s$ and $2s2p^3 3p$ configurations lie close to the upper levels of the $2s^2 2p^2 3s$, $2s^2 2p^2 3p$ and $2s^2 2p^2 3p$ configurations, interacting with them. Mason and Bhatia performed their *collisional* calculations including only the $2s^2 2p^3$, $2s2p^4$, $2s^2 2p^2 3s$, $2s^2 2p^2 3p$ configurations with $2p^5$ as correlation. Thus our present target represents a significant improvement.

In any case, the most important change compared to the previous work is the presence of the resonance contributions made possible by the use of the close-coupling approximation. This is illustrated in Fig. 5 in which the collision strength for the $2s^2 2p^3\ {}^4S^\circ_{3/2}$–$2s^2 2p^3\ {}^2D^\circ_{3/2}$ forbidden transition is displayed. This cross section is dominated by resonances while the *background* cross section is given correctly by the distorted wave calculations. The resonances lead to a considerable enhancement in the collision rates compared to the earlier results.

The target information, energies and oscillator strengths, given in Sect. 2, indicates that the wavefunctions provide an accurate description of the levels included in the present target. Thus the most significant factor limiting the accuracy of the current data is the omission of resonant contributions from higher lying configurations. This will not have a large effect on the transitions among the $n = 2$ levels at the temperatures of interest and they may be expected to be accurate to better than 20%. On the other hand, errors for transitions into the $n = 3$ states will be larger because of this.

We hope to perform more extensive calculations for this ion in the future which will reduce the uncertainties in the cross sections further. However, our more immediate goal will be to apply these methods to other iron group ions of the same isoelectronic sequence.

Acknowledgements. The present calculations were carried out on the Cray T-90 and the Fujitsu VPP700 at the Leibniz-Rechenzentrum of the Bayerische Akademie der Wissenschaften. The generous allocation of computer time and resources is gratefully acknowledged.

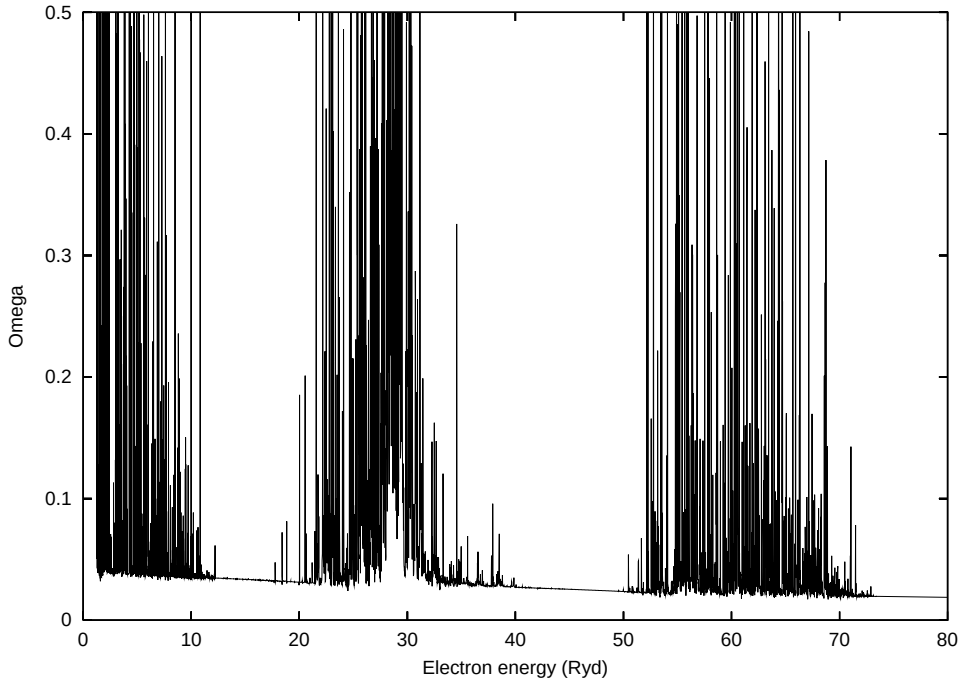

Fig. 5. Collision strength for the $2s^2 2p^3\ {}^4S^\circ_{3/2}$–$2s^2 2p^3\ {}^2D^\circ_{3/2}$ transition as a function of energy. Note the contribution from the resonances.

Table 4. Effective collision strengths for a temperature of $\log T = 6.9$.

1	2	5.900E-02	1	3	5.820E-02	1	4	2.062E-02	1	5	3.034E-02	1	6	4.827E-01
1	7	3.435E-01	1	8	1.787E-01	1	9	1.743E-02	1	10	3.761E-03	1	11	7.064E-03
1	12	2.842E-02	1	13	2.415E-03	1	14	7.177E-04	1	15	1.724E-04	2	3	7.950E-02
2	4	4.413E-02	2	5	5.374E-02	2	6	5.151E-02	2	7	1.209E-02	2	8	8.125E-03
2	9	5.741E-01	2	10	1.216E-02	2	11	1.897E-01	2	12	1.094E-01	2	13	8.025E-02
2	14	2.070E-03	2	15	1.270E-03	3	4	3.625E-02	3	5	1.028E-01	3	6	4.075E-02
3	7	1.009E-02	3	8	2.278E-03	3	9	1.297E-02	3	10	7.175E-01	3	11	1.847E-03
3	12	8.218E-01	3	13	2.130E-03	3	14	2.428E-03	3	15	1.193E-03	4	5	3.635E-02
4	6	3.823E-03	4	7	4.945E-03	4	8	1.013E-02	4	9	6.438E-02	4	10	6.044E-03
4	11	2.314E-01	4	12	9.678E-02	4	13	1.692E-02	4	14	6.716E-04	4	15	6.900E-04
5	6	1.305E-02	5	7	2.330E-02	5	8	4.691E-03	5	9	2.356E-02	5	10	2.389E-01
5	11	2.264E-02	5	12	1.307E-01	5	13	4.561E-01	5	14	1.253E-03	5	15	2.112E-03
6	7	7.038E-02	6	8	2.626E-02	6	9	3.074E-02	6	10	5.902E-02	6	11	1.305E-02
6	12	1.570E-02	6	13	6.738E-03	6	14	3.202E-02	6	15	3.087E-03	7	8	3.510E-02
7	9	2.890E-02	7	10	2.900E-02	7	11	9.942E-03	7	12	1.326E-02	7	13	7.798E-03
7	14	1.845E-02	7	15	5.318E-03	8	9	1.427E-02	8	10	1.270E-02	8	11	5.438E-03
8	12	7.453E-03	8	13	4.439E-03	8	14	7.223E-03	8	15	4.976E-03	9	10	5.677E-02
9	11	2.698E-02	9	12	5.351E-02	9	13	1.858E-02	9	14	2.328E-01	9	15	2.130E-01
10	11	3.322E-02	10	12	5.799E-02	10	13	2.441E-02	10	14	6.116E-01	10	15	7.325E-03
11	12	2.556E-02	11	13	1.742E-02	11	14	2.142E-01	11	15	2.245E-02	12	13	4.422E-02
12	14	8.550E-01	12	15	3.318E-01	13	14	7.540E-02	13	15	4.257E-01	14	15	5.687E-02

References

Arnaud, M., & Rothenflug, R. 1985, A&AS, 60, 425

Berrington, K. A., Burke, P. G., Le Dourneuf, et al. 1978, Comput. Phys. Commun., 14, 367

Berrington, K. A., Eissner, W. B., & Norrington, P. H. 1995, Comput. Phys. Commun., 92, 290

Bhatia, A. K., & Mason, H. E. 1980, A&A, 83, 380

Burgess, A., & Tully, J. A. 1992, A&A, 254, 436

Burke, V. M., & Seaton, M. J. 1986, J. Phys. B, 19, L527

Butler, K., & Zeippen, C. J. 2000, A&AS, 143, 483

Eissner W., Galavis, M. E., Mendoza, C., et al. 1999, A&AS, 136, 385

Eissner, W., Jones, M., & Nussbaumer, H. 1974, Comput. Phys. Commun., 8, 270

Hummer, D. G., Berrington, K. A., Eissner, W., et al. 1993, A&A, 279, 298

Mason, H. E., & Bhatia, A. K. 1983, A&AS, 52, 181

Nussbaumer, H., & Storey, P. J. 1978, A&A, 64, 139

Phillips, K. J. H., Leibacher, J. W., Wolfson, C. J., et al. 1982, ApJ, 256, 774

Sugar, J., & Corliss, C. 1985, J. Phys. Chem. Ref. Data 14, Suppl., 2, 498

Zhang, H. L., & Sampson, D. H. 1999, ADNDT, 72, 153